Chapter 1

Introduction

The basic features of wave propagation in the half-space with soil medium are discussed. A review is presented of the various methods used in investigating the soil vibrations, including the analytical methods, field measurements, empirical prediction models, and numerical methods of simulation. Particular emphasis is placed on the vibrations induced by trains moving on the ground or through underground tunnels. Also summarized are the methods of isolation for ground-borne vibrations and the evaluation criteria adopted by different countries.

1.1 Ground-Borne Vibrations

Railway trains have been a major form of mass public transportation in the world for more than one and half centuries. There exists a wide variety of railway trains, ranging from the traditional freight and passenger trains to subway trains and high-speed trains. Different types of railway trains should meet different service, safety and environmental considerations. Even though great progress has been made in air transportation in the past century for long-distance, international, and trans-ocean travels, the status of railways as a key transportation tool for medium and short-distance travels remains the same. As a matter of fact, almost all major cities in the world have built their own subway systems, while high-speed railways have become increasingly popular in Asian and European countries following the launch of the *bullet train* in Japan in 1964.

Owing to the popularity of subways and high speed railways worldwide, most major cities have encountered the problem that railway lines have inevitably come close to some vibration-sensitive residential areas, laboratories, hospitals, high-precision science parks or telecommunication buildings. Although the vibrations induced by passing trains may not result in structural damages on adjacent buildings, they are known to cause the malfunctioning of some high-precision instruments or facilities housed in the buildings and to result in higher imperfection rates for integrated circuit production lines, while becoming a source of continuous annoyance to the occupants of buildings located alongside the railways. It should be mentioned that the effect of vibration on human comfort and annoyance is a very complex problem, which cannot be specified solely by the magnitude of monitored vibrations alone.[1] Recently, more and more vibration data have been collected from existing railway lines. Partly due to stricter environmental considerations, the problem of train-induced vibrations and their influence on human comfort and operation of sensitive equipment has received increasing attention from engineers, researchers and urban transportation planners in recent years.

The ground vibration induced by moving trains is a complicated dynamic problem. Vibrations of various sorts can be generated by the passage of trains due to the surface irregularities of wheels and rails, the rise and fall of the axles over sleepers. They can be transmitted through the track structure, including the rails, sleepers, ballast and sub-layers, propagate as waves through the soil medium, and then reach the buildings located nearby, creating a sense of discomfort to the occupants there. It should be noted that even for a train with perfect wheels moving over smooth rails, i.e., with no imperfections or unevenness in components such as wheels and rails, vibrations can still be generated by the regular repetitive action of the moving loads of the train.

Four major phases can be identified for the transmission of vibrations from the moving train through the railway, ties and subsoils to the neighboring structures: (a) *Generation*, i.e., the excitation caused by the regular repetitive action of moving wheel loads on the rails, plus the impact caused by the rotating wheels over the rails due to surface irregularities; (b) *Transmission*, i.e., the propagation of waves through

[1] Both the vibration and noise induced by passing trains may be of concern in this regard.

the surrounding soils; (c) *Reception*, i.e., the vibrations received by nearby buildings; and (d) *Interception*, i.e., the reduction in vibrations through implementation of wave barriers, such as piles, trenches, isolation pads, etc.

In each phase, various factors may affect the levels of vibrations to certain extents. The primary factors entering into consideration include the train type, train speed, track design, embankment design, ground condition, building foundation, building type, and the distance between the railway and buildings. The lack of an in-depth understanding of all these factors makes it difficult to simulate the problem in an accurate manner. Under certain circumstances, however, it is possible to estimate the levels of ground vibrations transmitted from the railways or traffic roads using a combination of empirical and theoretical formulas that have been made available.

Previously, the problem of ground-borne vibrations has been dealt with using mainly four different approaches, i.e., the *analytical approaches*, *field measurements*, *empirical prediction models*, and *numerical simulation*. In this chapter, a general survey will be given of each of the four approaches, followed by two separate sections each on the isolation of traffic-induced vibrations using some control devices and the evaluation criteria of vibrations adopted in different countries. All in all, we realize that research on train-induced vibrations has been voluminous and will grow continuously. It is almost impossible to come up with a compressive listing of all the relevant papers. We also realize that some of the research works were not available in English, especially those from Europe and Japan, where high-speed railways and subways have been put into operation for several decades. Under such a constraint, only papers that are readily available to the writers and have been written in English or Chinese will be cited in this chapter.

1.2 Analytical Approaches

By an analytical approach, one uses the theoretical models to describe the wave propagation characteristics of the source-path-receiver system. Because of the simplifications inevitably made in the modeling, exact closed-form solutions for most practical problems are at present not available. However, even for the limited number of ideal cases studied, the solutions obtained by previous researchers did provide us with a general picture of the key parameters involved. Solutions such as these are useful references for validating the results obtained by other numerical approaches.

1.2.1 *Classical theory of wave propagation*

The pioneering work of Lamb (1904) contained most of the elements that are essential to analytical studies of the sources and transmission paths in soils. In this work, Lamb investigated the disturbance generated in an elastic medium due to an impulsive force applied along a line or at a point on the semi-infinite surface or inside an unbounded full space. These solutions can be extended to yield the steady-state solutions for the cases with moving loads at constant speeds, if a new coordinate system moving synchronously with the loads is adopted. In reality, Lamb's solutions were also used by researchers as the basis in developing empirical prediction models. For the reasons stated, major features of the elastic half-space problem subjected to a point or line load, as was studied by Lamb, should be further explained. In this regard, it is realized that the same problems were analyzed subsequently by a number of researchers at different times, including, in particular, Ewing *et al.* (1957), Fung (1965), Graff (1973), and Achenbach (1976), among others. In the two somewhat tutorial papers presented by Gutowski and Dym (1976) and Dawn and Stanworth (1979), some major features of the elastic half-space problem were thoroughly discussed.

The governing equations for a homogenous isotropic solid can be written in terms of displacements **u** as

$$(\lambda + \mu)\nabla\nabla \cdot \mathbf{u} + \mu\nabla^2\mathbf{u} + \rho\ \mathbf{f} = \rho\ \ddot{\mathbf{u}}, \tag{1.1}$$

where λ and μ, the *Lamé constants*, are the elastic constants for the material; the latter is also known as the *shear modulus* and denoted as G in later chapters. Both constants can be expressed in terms of other elastic constants, such as *Young's modulus E*, *Poisson's ratio* ν, and the bulk modulus $\boldsymbol{K}$ (Graff, 1973):

$$E = \frac{\mu(3\lambda + 2\mu)}{\lambda + \mu}, \tag{1.2a}$$

$$\nu = \frac{\lambda}{2(\lambda + \mu)}, \tag{1.2b}$$

$$K = \lambda + \frac{2}{3}\mu. \tag{1.2c}$$

In Eq. (1.1), ρ is the mass density per unit volume of the material and **f** is the body force per unit mass of the material. Consider the governing equations in the absence of body forces. By performing the vector operation of divergence, one obtains

$$(\lambda + \mu)\nabla \cdot (\nabla\nabla \cdot \mathbf{u}) + \mu\nabla \cdot (\nabla^2\mathbf{u}) = \rho\nabla \cdot \ddot{\mathbf{u}}. \tag{1.3}$$

Since $\nabla \cdot \nabla = \nabla^2$ and $\nabla \cdot (\nabla^2\mathbf{u}) = \nabla^2(\nabla \cdot \mathbf{u})$, the preceding equation can be reduced to

$$(\lambda + 2\mu)\nabla^2\mathbf{\Delta} = \rho\frac{\partial^2\mathbf{\Delta}}{\partial t^2}, \tag{1.4}$$

where $\mathbf{\Delta} = \nabla \cdot \mathbf{u}$ is the *dilation* of the material. Equation (1.4) can be recognized as the *wave equation*, expressible in the following form:

$$\nabla^2\mathbf{\Delta} = \frac{1}{c_P^2}\frac{\partial^2\mathbf{\Delta}}{\partial t^2}, \tag{1.5}$$

where the *propagation velocity* c_P is given by

$$c_P = \sqrt{\frac{\lambda + 2\mu}{\rho}}. \tag{1.6}$$

We thus conclude that *dilatational waves* will propagate at the velocity c_P in the solid.

We now perform the operation of curl on the governing equation in Eq. (1.1) neglecting the body forces. Since the curl of the gradient of a scalar is zero, we obtain

$$\mu\,\nabla^2\boldsymbol{\omega} = \rho\frac{\partial^2\boldsymbol{\omega}}{\partial t^2}, \tag{1.7}$$

where $\boldsymbol{\omega} = \nabla \times \mathbf{u}/2$ is the rotation vector. The preceding equation can also be expressed in the form of *vector wave equation*, i.e.,

$$\nabla^2 \boldsymbol{\omega} = \frac{1}{c_S^2} \frac{\partial^2 \boldsymbol{\omega}}{\partial t^2}, \tag{1.8}$$

where the propagation velocity c_S is given by

$$c_S = \sqrt{\frac{\mu}{\rho}}. \tag{1.9}$$

Thus, *rotational waves* will propagate at velocity c_S in the medium.

We have found that waves may propagate through the interior of an elastic solid at two different speeds c_P and c_S. Dilatational waves, involving no rotation, propagate at the speed c_P, while rotational waves, involving no volume changes, propagate at the speed c_S. In general, the speed for the dilatational waves, c_P, is greater than that for the rotational waves, c_S, as can be observed by comparing Eqs. (1.5) with (1.8). A variety of terminology exists for the two types of waves. Dilatational waves are also known as *irrotational* or *primary* (*P*) *waves*, and the rotational waves as *equi-voluminal*, *distortional*, or *secondary* (*S*) *waves*. The P and S wave designations have arisen mainly from the seismological society. Other designations frequently used for the P waves are *longitudinal* or *compressional waves* and for the S waves are *transverse* or *shear waves*.

When an elastic wave encounters a boundary between two media, energy is reflected from and refracted across the boundary. If the boundary is a free surface, no refraction can occur. A major feature of the wave-boundary interaction process is mode conversion.

Except the two types of waves mentioned above, a third type of waves may exist whose effects are confined closely to the surface. Such waves were called *Rayleigh* (*R*) *waves*, as they were first investigated by Lord Rayleigh, who showed that their effect decreases rapidly with depth and their velocity of propagation is somewhat less than that of shear waves. The Rayleigh wave velocity c_R can be approximately related to the shear wave velocity c_S as

$$\frac{c_R}{c_S} = \frac{(0.87 + 1.12\nu)}{(1+\nu)}. \tag{1.10}$$

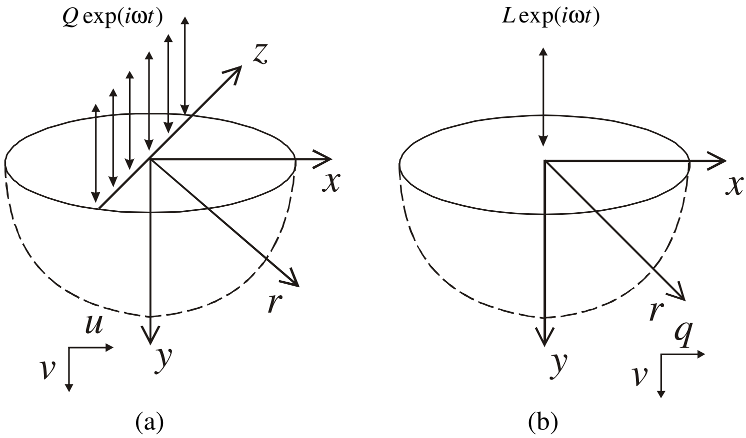

Fig. 1.1 Classical Lamb's problems with harmonic: (a) line load; (b) point load.

To honor the contribution of Lamb to the classical theory of wave propagation, the problems studied by Lamb have been named after him and grossly referred to as *Lamb's problems*.

Let us consider two typical Lamb's problems that are central to the present study in Fig. 1.1, in which parts (a) and (b) show a uniform elastic half-space subjected to a harmonic line load and an oscillating point load, respectively. Since the early work of Lamb, the same problems have been studied again by many researchers, including Ewing *et al.* (1957), Graff (1973), and Achenbach (1976), among others.

For the case of a harmonic line load $Q\exp(i\omega t)$ applied on the surface of the half-space, i.e., case (a) in Fig. 1.1, where Q is the magnitude of the applied load and ω the frequency of excitation, the horizontal displacement u and vertical displacement v on the surface ($y = 0$) of the half-space can be given as follows (Ewing *et al.*, 1957):

$$u = (Q/\mu)\Big\{-H\exp\left[i(\omega t - k_R x)\right] + C\left(k_P x\right)^{-3/2}\exp\left[i\left(\omega t - k_P x\right)\right] + D\left(k_S x\right)^{-3/2}\exp\left[i\left(\omega t - k_S x\right)\right] + \cdots\Big\}, \tag{1.11}$$

$$v = (Q/\mu) = \Big\{-iK\exp\left[i(\omega t - k_R x)\right] + C_1\left(k_P x\right)^{-3/2}\exp\left[i\left(\omega t - k_P x\right)\right] + D_1\left(k_S x\right)^{-3/2}\exp\left[i\left(\omega t - k_S x\right)\right] + \cdots\Big\}, \tag{1.12}$$

where $\cdots$ represents the higher order terms of the solutions, which can be neglected for farther distance x. The factors C, D, C_1, D_1, H and K depend on the wave numbers $k_S = \omega / c_S$, $k_P = \omega / c_P$ and $k_R = \omega / c_R$, but not on the distance x from the source:

$$C = -i\sqrt{\frac{2}{\pi}}\frac{k_P^3 k_S^2 \left(k_S^2 - k_P^2\right)^{1/2}}{\left(k_S^2 - 2k_P^2\right)^3}\exp\left(-i\frac{\pi}{4}\right), \tag{1.13a}$$

$$D = \sqrt{\frac{2}{\pi}}\sqrt{1 - \frac{k_P^2}{k_S^2}}\exp\left(-i\frac{\pi}{4}\right), \tag{1.13b}$$

$$C_1 = \frac{i}{2}\sqrt{\frac{2}{\pi}}\frac{k_P^2 k_S^2}{\left(k_S^2 - 2k_P^2\right)^2}\exp\left(-i\frac{\pi}{4}\right), \tag{1.13c}$$

$$D_1 = 2\sqrt{\frac{2}{\pi}}\left(1 - \frac{k_P^2}{k_S^2}\right)\exp\left(-i\frac{\pi}{4}\right), \tag{1.13d}$$

$$H = -\frac{k_R\left(2k_R^2 - k_S^2 - 2\sqrt{k_R^2 - k_P^2}\sqrt{k_R^2 - k_S^2}\right)}{F'\left(k_R\right)}, \tag{1.13e}$$

$$K = -\frac{k_S^2\sqrt{k_R^2 - k_P^2}}{F'\left(k_R\right)}. \tag{1.13f}$$

In Eqs. (1.13e) and (1.13f),

$$F'\left(k_R\right) = \left.\frac{dF(k)}{dk}\right|_{k=k_R}, \tag{1.14}$$

where $F(k)$ is the *Rayleigh function*,

$$F\left(k\right) = \left(2k^2 - k_S^2\right)^2 - 4k^2\sqrt{k^2 - k_P^2}\sqrt{k^2 - k_S^2}. \tag{1.15}$$

In Eqs. (1.11) and (1.12) for the displacement responses, the first, second, and third terms represent the contribution of the R-, P-, and S-waves, respectively. Clearly, for the case of harmonic line load considered, the R-waves do not suffer from any geometric attenuation on the ground surface, while both the P- and S-waves show a rate of attenuation proportional to $x^{-3/2}$.

Now, let us consider the case of a point load $L\exp(i\omega t)$ applied on the surface of the half-space, as shown in Fig. 1.1(b), where L denotes the magnitude of the applied load. The displacements of the half-space can be derived in the cylindrical coordinates, since they are symmetrical about the y-axis penetrating into the body. According to Ewing *et al.* (1957), the radial displacement q and vertical displacement v on the ground surface ($y = 0$) are

$$q = \frac{L}{\mu}\left\{ -ik_R H \sqrt{\frac{1}{2\pi k_R x}} \exp\left[i\left(\omega t - k_R x - \frac{\pi}{4} \right) \right] + \frac{M}{(k_P x)^2} \exp[i(\omega t - k_P x)] \right.$$
$$\left. + \frac{N}{(k_S x)^2} \exp[i(\omega t - k_S x)] + \cdots \right\}, \tag{1.16}$$

$$v = \frac{L}{\mu}\left\{ k_R K \sqrt{\frac{1}{2\pi k_R x}} \exp\left[i\left(\omega t - k_R x - \frac{\pi}{4} \right) \right] + \frac{M_1}{(k_P x)^2} \exp[i(\omega t - k_P x)] \right.$$
$$\left. + \frac{N_1}{(k_S x)^2} \exp[i(\omega t - k_S x)] + \cdots \right\}, \tag{1.17}$$

where x denotes the radial distance from the point load to the point of concern. Again, the first terms of Eqs. (1.16) and (1.17) represent the contribution of the R-waves. However, for the case of a point load applied on the half-space, the R-waves attenuate along the surface inversely proportional to the square root of the distance from the source, i.e., with a decaying rate proportional to $x^{-1/2}$. The remaining terms in the preceding two equations represent the contribution of the P- and S-waves, where M, N, M_1 and N_1 depend on the wave numbers k_S and k_P, but not on the distance x. As can be seen, the amplitudes of P- and S-waves diminish with the distance as a function of x^{-2} on the ground surface. Thus, the *geometric attenuation* of the P- and S-waves on the surface is more severe than that of the R-waves.

Concerning the interior of the half-space, Graff (1973) showed that for the case with a point load applied on the half-space, both the P- and S-waves decay at a rate proportional to r^{-1}, where r is the distance from the source to the point of concern in the interior of the half-space. In contrast, the response for the case of a line load is typical of cylindrical energy spreading, for which the attenuation rate for the P- and S-waves is proportional to $r^{-1/2}$ in the interior of the half-space.

As can be seen from the above discussions, the R-waves have a relatively good capability in travelling for a long distance on the surface of the half-space, but the same is not true for the P- and S-waves. In other words, the R-waves exist primarily near the surface, but the P- and S-waves have a better capability in penetrating through the interior of the half-space. For this reason, the R-waves have also been referred to as the *surface waves*, and the P- and S-waves as the *body waves*.

1.2.2 *Elastic medium subjected to moving loads*

With the continuous increase in the moving speed of passenger trains worldwide, the effect of speed of the moving loads has drawn much more attention from researchers than ever. One of the major concerns on the moving speed of passenger trains is the shock waves that may be produced as the train passes through some elastic barriers. It is well known that when an airplane passes through the sound barrier, the so-called *Mach radiation* of shock waves will occur. Likewise, when a moving train surpasses the *characteristic speed* of the waves of the soil medium, significant radiation effect can be expected for the ground motions. Obviously, the classical theory of wave propagation becomes insufficient, as no account has been taken of the effect of speed of the moving objects with respect to the soil medium.

After the classical questions associated with wave propagation had been answered to a certain level of satisfaction, scientists working on soil dynamics began to extend the framework established primarily by Lamb to the analysis of moving load problems. Consider an elastic medium subjected to a load moving at speed c. The solution for such a problem can be divided into three speed ranges:

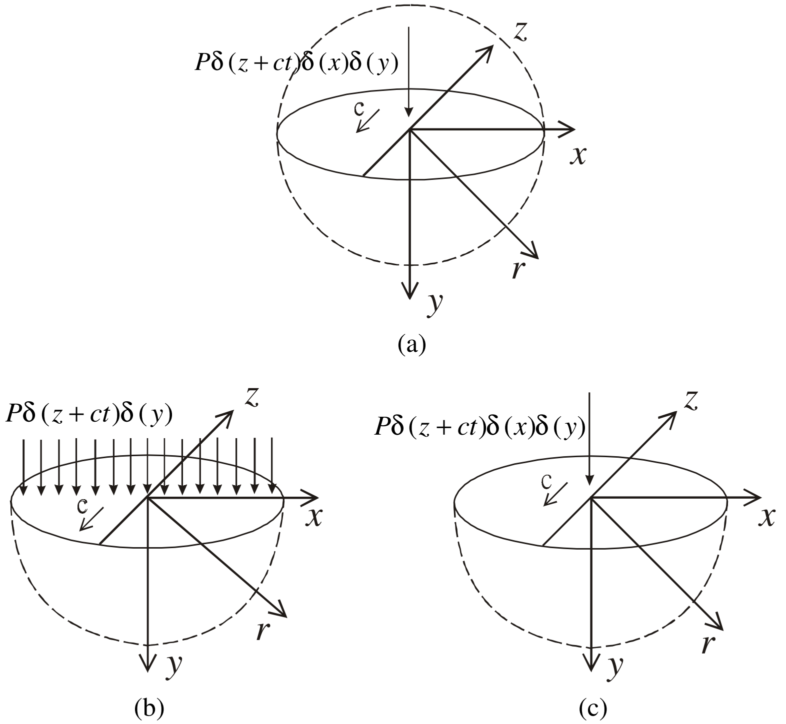

Fig. 1.2 Elastic body subjected to a moving load: (a) unbounded elastic body with point load; (b) elastic half-space with line load; (c) elastic half-space with point load.

(a) *Sub-critical speed* ($c < c_S$): The load is moving at a speed less than the S-wave speed of the elastic medium;
(b) *Tran-critical speed* ($c_S < c < c_P$): The load moves at a speed greater than the S-wave speed, but smaller than the P-wave speed; and
(c) *Super-critical speed* ($c_P < c$): The moving speed of the load is greater than the P-wave speed.

In the literature, terms such as *sub*-, *trans*-, and *super-sonic speeds* have also been used. However, due to the fact that the original meaning of sonic speed refers to the speed of sound or air, which is not the case encountered herein, we prefer to use the terms *critical speeds* to refer to the speeds of soils or the ground in this book. Besides, for problems where the surface waves play a much more important role than the body waves, e.g., those studied in Chapters 8 and 9, the Rayleigh wave speed may be chosen as the critical speed instead.

With regard to the effect of speed of the moving loads, three problems have been studied by researchers, as depicted in Figs. 1.2(a)-(c), in which part (a) shows an *elastic unbounded body* subjected to a moving point load, and parts (b) and (c) show an elastic half-space subjected to a moving line load and a moving point load, respectively. All the three cases are not purely of mathematical interest, but may have some implications in reality. For instance, the problem in Fig. 1.2(a) may find applications in computation of the response of soils around a tunnel through which the train passes. The problem in Fig. 1.2(c) represents the effect of an at-grade moving train. As far as the three ranges of moving speeds are concerned, there is a total of nine solutions for the three problems considered. However, only the three solutions for problem (a) are available in closed form. The solutions to problems (b) and (c) have to be computed by numerical procedures. Major features for the three problems will be briefly summarized in the following.

1.2.2.1 *Elastic unbounded body subjected to a moving point load*

Frýba (1972) analyzed the response of the unbounded elastic body in Fig. 1.2(a) to a moving point load by the technique of triple Fourier integral transformation. The solution obtained by Frýba (1972) for the vertical displacement v in the elastic body at $t = 0$ subjected to a point load P with speed c moving in the negative z-direction is

- Sub-critical speed:

$$v = \frac{P}{4\pi\mu {M_2}^2}\left[\frac{{M_2}^2}{R_2} + \frac{x^2}{r^4}\left(R_2 - R_1\right) - \frac{y^2 z^2}{r^4}\left(\frac{1}{R_2} - \frac{1}{R_1}\right)\right], \tag{1.18a}$$

- Trans-critical speed:

$$\begin{aligned} v = \frac{P}{4\pi\mu {M_2}^2}\Bigg\{&\frac{{M_2}^2}{R_2}H\left(z - a_2 r\right) + \frac{x^2}{r^4}\left[R_2 H\left(z - a_2 r\right) - R_1\right] \\ &- \frac{y^2 z^2}{r^4}\left[\frac{1}{R_2}H\left(z - a_2 r\right) - \frac{1}{R_1} + \frac{a_2 r R_2}{z^2}\delta(z - a_2 r)\right]\Bigg\}, \end{aligned} \tag{1.18b}$$

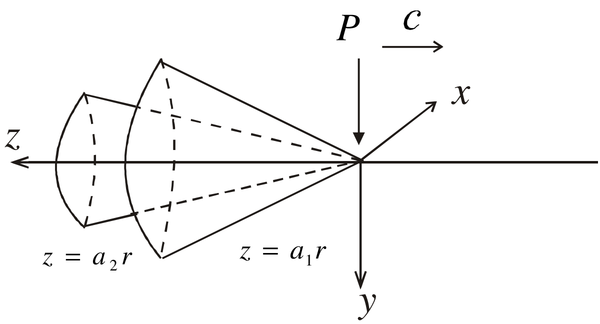

Fig. 1.3 Two Mach cones existing at super-critical speeds.

- Super-critical speed:

$$v = \frac{P}{4\pi\mu M_2{}^2}\left\{\frac{M_2{}^2}{R_2}H\left(z-a_2r\right)+\frac{x^2}{r^4}\left[R_2H\left(z-a_2r\right)\right.\right.$$
$$\left.-R_1H\left(z-a_1R\right)\right]-\frac{y^2z^2}{r^4}\left[\frac{1}{R_2}H\left(z-a_2r\right)-\frac{1}{R_1}H(z-a_1r)\right.$$
$$\left.\left.+\frac{r}{z^2}\left(a_2R_2\delta(z-a_2r)-a_1R_1\delta(z-a_1r)\right)\right]\right\}, \tag{1.18c}$$

where

$$a_i^2 = \left|1-M_i^2\right|, \quad r^2 = x^2+y^2, \quad R_i^2 = z^2+(1-M_i^2)r^2, \tag{1.19}$$

for i = 1,2. Here, $M_1 = c/c_P$ and $M_2 = c/c_S$ denote the *Mach numbers* related to the P- and S-waves, respectively, μ is the shear modulus for the elastic body, $H(x)$ the Heaviside function, and $\delta(x)$ the Dirac function.

As can be seen from Eq. (1.18), the vertical displacement is symmetrical about the x axis for the sub-critical speed range. But when the load speed exceeds the speeds of the P- or S-waves, the effects of the corresponding waves are confined to a region of the solid bounded by a trailing *Mach cone* with apex at the loading point and moving with it. The P-wave Mach cone can be written as $z = a_1r$ and the S-wave Mach cone as $z = a_2r$ (see Fig. 1.3). From Eq. (1.18c), one observes that no vibrations will be induced ahead of the P-wave front.

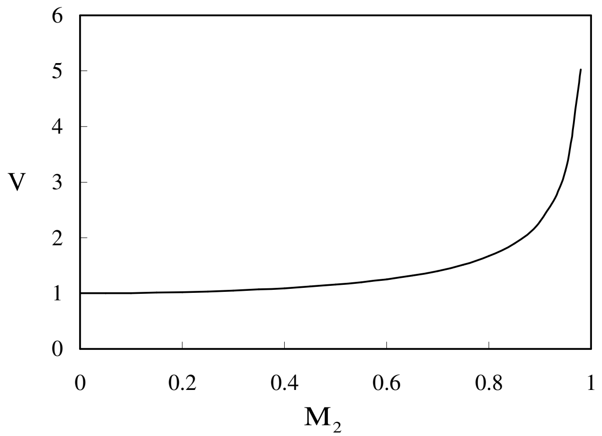

Fig. 1.4 Maximum vertical displacement versus the S-wave Mach number for an unbounded elastic body subjected to a moving point load.

Based on Eq. (1.18a) for the sub-critical speed range, the maximum vertical displacement v at the point (x = 0 m, y = 1 m, z = 0 m) was plotted with respect to the S-wave Mach number M_2 in Fig. 1.4, where the displacements have been given in a normalized form, i.e., $V = (4\pi\mu/P)v$. As can be seen, the displacement increases with the speed of the moving load. The variation appears to be gradual in the range with $M_2 < 0.6$, but for the range $M_2 > 0.6$, the displacement increases dramatically following the increase of M_2. Also, there exists a tendency that as the moving speed of the load approaches the S-wave speed, i.e., as M_2 approaches unity, the displacement becomes infinite.

1.2.2.2 *Elastic half-space subjected to a moving line load*

A general integral solution was given by Sneddon (1951) for the two-dimensional problem of a line load moving with a uniform sub-critical speed over the surface of a uniform elastic half-space. Cole and Huth (1958), Fung (1965), and Frýba (1972) considered the same problem for a normal line load and obtained solutions for the sub-, trans-, and super-critical speeds. The transient problem for a line load that suddenly appears on the surface of an elastic half-space and then moves with constant speed was considered by Payton (1967). From the aforementioned works, it is observed that if the load moves steadily at a speed equal to the R-wave speed, the response will become infinitely large. For the load moving at a super-critical speed, two *Mach planes* ($z = a_1 y$ and $z = a_2 y$) with singularities in displacement, instead of the two Mach cones, will occur.

1.2.2.3 *Elastic half-space subjected to a moving point load*

Eason (1965) studied the three-dimensional steady-state problem for a uniform half-space subjected to a point load moving at constant speeds. Besides the point load, Eason also considered the case of moving loads distributed over a circular or rectangular area. The governing equations were solved by means of integral transform, with the resulting multiple integrals reduced to single finite integrals for the sub-critical speed case. Gakenheimer and Miklowitz (1969) derived the transient displacements for the interior of an elastic half-space under a normal point load that is suddenly applied and then moves at a constant speed on the free surface. All the sub-, trans-, and super-critical speed cases were studied, while the inverse transform is evaluated by the Carniard-de Hoop technique. The steady-state response for the same problem was also given by Frýba (1972) in integral form. Using a method similar to Eason's (1965), Alabi (1992) studied the response due to an oblique moving point load on the free surface. By numerical integration, a parametric study was performed to investigate the effects of the load speed, distance and ground depth for the sub-critical speed case.

Following generally the procedure proposed by Luco and Aspel (1983), the steady-state displacements and stresses were solved by de Barrors and Luco (1994) for a multi-layered viscoelastic half-space due to a buried or surface point load moving along a horizontal straight line with sub-, trans-, or super-critical speed. The effect of layering was considered by using an exact factorization for the displacement and stress fields in terms of the generalized transmission and reflection coefficients. By the Fourier transform and a special integration scheme, Yeh *et al.* (1997) obtained the response of an elastic half-space to a moving point load for the sub-critical speed case. In the study by Lieb and Sudret (1998), the inverse transformation was performed by a decomposition in wavelets and the layered half-space was modeled by one-dimensional finite elements for the vertical direction in the transformed domain. Grundmann *et al.* (1999) studied the response of a layered half-space to a single moving periodic load as well as a simplified train load.

By the Fourier transform and a special integration technique, Hung and Yang (2001) proposed an analytical procedure for studying the mechanism of wave propagation for a uniform elastic half-space under the moving loads with static and dynamic components, considering four different types of moving load patterns. Also presented is a parametric study to investigate the effect of moving loads of the sub-, trans-, and super-critical speed ranges on the response of the underlying soils. Sheng *et al.* (2004) proposed a ground vibration model comprising the vehicles, track and ground for investigating the ground vibration in the presence of rail irregularities.

1.2.3 *Beam on elastic half-space subjected to moving loads*

As mentioned above, when an object moves at a speed greater than the wave speed of the surrounding medium, a *Mach cone* that moves with the object will be generated. For the case of moving trains, the moving load is first acting on the rails and then transmitted via the track and foundations to the underlying half-space. Obviously, the *characteristic speed* of the rails and foundations should be taken into account. In the literature, the supporting railroad track has been modeled as a beam resting on a *Winkler foundation* by a number of researchers. For instance, Frýba (1972) presented a detailed solution for the problem of a constant load moving along an *infinite beam* on an elastic foundation, considering all possible speed ranges and values of viscous damping. By the concept of *equivalent stiffness* for the supporting structure, a *critical speed* was identified for the moving load, at which the response of the beam becomes infinite. Such a speed corresponds exactly to the propagation speed of waves in the beam. For a load with speeds smaller than the critical speed, the largest amplitude of waves occurs near the point of loading. On the other hand, for a load with speeds greater than the critical speed, the waves moving ahead of the load are of small wavelengths and amplitudes compared with those behind the load.

The critical speed for a *Bernoulli-Euler beam* is the lowest bending wave speed, which can be given as

$$c_{cr} = \sqrt[4]{\frac{4sEI}{m^2}} \tag{1.20}$$

in which m is the mass per unit length, E the elastic modulus, I the moment of inertia of the beam, and s the coefficient of the Winkler foundation, usually assumed to be a constant. Similar results were obtained by Duffy (1990) in his study for the vibrations arising when a moving, vibrating mass passes over an infinite railroad track lying on a Winkler foundation.

By substituting the material properties for typical railroads into Eq. (1.20), researchers concluded that coincidence of the train speed with the critical speed is extremely unlikely (Frýba, 1972; Heckl *et al.*, 1996). However, the accuracy of these results can be largely influenced by the value used for the foundation coefficient s, which in practice is difficult to determine. Dieterman and Metrikine (1996, 1997) and Metrikine and Dieterman (1997) conducted a series of analysis to derive the *equivalent stiffness* of an elastic half-space interacting with a Bernoulli-Euler beam of finite width. They found that the equivalent stiffness depends mainly on the frequency and wave number of the beam. With this equivalent stiffness taken into account, the analysis indicated that there exist two *critical speeds*. One corresponds to the R-wave speed and the other is somewhat smaller than the R-wave speed. Both speeds can result in severe amplification of the displacement of the beam. Later, Lieb and Sudret (1998) performed a similar analysis and found that severe displacements can be observed on the half-space underlying the rails at the critical speeds as well. Metrikine *et al.* (2001) used a similar track model overlying a visco-elastic half-space to theoretically investigate the phenomenon of *visco-elastic drag* associated with the excitation of ground waves by a high-speed train.

Suiker *et al.* (1998) further studied the critical behavior of a Timoshenko-beam-half-space system under the moving load. If the highway traffic, instead of the railroad traffic, is considered, then it is more proper to use a model with a plate on elastic foundations. Kim and Roësset (1998) investigated the dynamic response of an *infinite plate* on an elastic foundation subjected to the moving load. The *critical speed* observed for such a case is

$$c_{cr} = \sqrt[4]{\frac{4sD}{m^2}}, \tag{1.21}$$

where D is the flexural rigidity of the plate, and m and s are the mass and stiffness of the foundation per unit area, respectively. Chen and Huang (2000) derived the critical velocities for both the Bernoulli-Euler and *Timoshenko beams* on *Winkler foundations*. It was found that the lowest bending wave speed of the rails and the Rayleigh wave speed of the ground are both over 500 km/hr for real situations.

1.2.4 *Tunnel structure subjected to moving loads*

Considering the interaction of a tunnel-soil-building system due to passing trains, Balendra *et al.* (1991) proposed a simple semi-analytical approach for predicting the level of ground-borne vibrations using a *substructure method*. The plane strain model they used comprises a rigid tunnel in the elastic half-space with a rigid embedded footing for supporting the building that was modeled as a lumped mass. The entire problem was decomposed into a foundation radiation boundary-value problem and a tunnel radiation boundary-value problem for the purpose of computing the impedance matrix for the entire system. By using the substructure method, the response of the building to the train loading was evaluated and compared with the allowable vibration limits.

To investigate the level of ground vibrations due to trains moving in a tunnel, Metrikine and Vrouwenvelder (2000a) proposed an analytical approach with a simple two-dimensional model consisting of a visco-elastic layer and a Bernoulli-Euler beam located inside the layer. Assuming the layer and the beam to be infinitely long in the longitudinal direction, they analyzed the surface vibration under three types of loadings moving along the beam, namely, constant, harmonically varying, and stationary random loads. Later, Metrikine and Vrouwenvelder (2000b) improved their procedure by using two identical Bernoulli-Euler beams connected by distributed springs, instead of a single beam. They recognized that the results obtained using such a two-dimensional model can be regarded as an upper estimate of the level of ground vibrations, as the practical situations may be quite different. Recently, Forrest and Hunt (2006a,b) proposed a three-dimensional analytical model for studying the train-induced ground vibration from a deep underground railway tunnel of circular cross section. The tunnel is assumed to be an infinitely long, thin cylindrical shell, whereas the surrounding soil is modeled by means of wave equations for an elastic continuum.

1.2.5 *Load generation mechanism*

For continuously welded rails and perfect wheels, the most important mechanism of excitation for ground vibrations by the moving trains is the *quasi-static pressure* exerted by the wheel axles onto the track. Such a pressure with certain patterns will move with the wheels. Krylov and Ferguson (1994) studied the ground vibration associated with railways by the *Green function* formalism, in which the deflection curve of a beam lying on a *Winkler foundation* and subjected to a stationary point load was adopted as the shape of the pressure generated by each wheel axle on the rails. The pressure generated by the wheel axle is distributed and radiated to the ground through the sleepers. By superposition of the elastic waves radiated by the sleepers caused by the passage of all the wheel axles and by taking into account the time lag between the forces and their locations in space, a load generating mechanism that is capable of simulating the influence of sleeper spacing, train length and train speed was constructed. As for the effect of subsoils, they utilized the results of the axisymmetric Lamb's problem for the half-space subjected to a vertical harmonic point load to determine the Green function, but considered only the contribution of the R-waves. Krylov (1995) further extended this analysis to studying the response caused by superfast trains, from which the *Mach radiation* can be observed as the train moves at a speed faster than the R-wave speed of the subsoil. In Takemiya's (1997) study, the same deflection curve was adopted to account for the quasi-static pressure generated by the wheel axles onto the ground. In this study, however, the sleeper spacing was not taken into account.

A *random vibration method* was used by Hunt (1991) to model the road traffic-induced ground vibration. In his study, vehicles were modeled as two-axle systems, each with four degrees of freedom, and the ground as a uniform elastic half-space with viscous damping. Based on Lamb's (1904) solution of the half-space response generated by a harmonic load on the surface, he derived the *frequency response function* for an elastic isotropic half-space. Later, Hunt (1996) extended the above approach to computation of the vibration transmission from railways into buildings using the random process. A similar method was adopted by Hao and Ang (1998) to estimate the *power spectral densities* of traffic-induced ground vibrations. In order to circumvent the difficulties associated with numerical integrations, they considered the contribution of the R-waves only and derived an approximate closed-form solution accordingly.

As far as the ground vibrations due to trains moving over multi-unit elevated bridges are concerned, a semi-analytical approach was proposed by Wu *et al.* (2002) with the following two features. First, the analytical solution of an elastically supported beam travelled by the moving loads is used to simulate the load-transmitting mechanism from the superstructure of the bridge. Second, the *Green's function* for an elastic half space under a point load is adopted to simulate the wave propagation behavior of the soil. For the kind of structures considered, such a semi-analytical approach is much more efficient for studying the ground-borne vibrations than those based on full numerical modeling. This approach was later extended by Wu and Yang (2004a,b) and Yang and Wu (2007) to the analysis of ground and building vibrations due to high speed trains of different types moving over multi-unit elevated bridges, in which the effect of elastic bearings, bridges piers, pile foundations, and foundation-soil interactions are all taken into account.

1.3 Field Measurement

By field measurement, the response of existing structures to various disturbances can be obtained directly. When sufficient measurements are taken, a data base can be compiled, by which the results can be analyzed using statistical approaches. These results can then be used as a basis for predicting the vibration levels of structures under similar conditions.

However, only after a statistically meaningful number of results have been made available for each case, can the effect of various parameter changes and corresponding vibration control measures be reliably predicted (Melke and Kraemer, 1983). Besides, successful site measurements of structures and ground vibrations require sophisticated electronic equipment. It is essential that a sufficient number of vibration sensors be deployed at different control points such that the representative response of wave transmission can be simultaneously measured. This will call for a number of high-quality long cables and remote amplifiers, if the data are to be transmitted to a central data logger without picking up extraneous noises (Newland and Hunt, 1991). Obviously, a thorough field measurement is the most time-consuming and expensive way among the four approaches mentioned above. Given below is a partial review of the experimental results obtained by some previous researchers for the railroads.

Dawn and Stanworth (1979) presented a few of the experimental studies conducted on the *British Railways*. Melke and Kraemer (1983) proposed an approach for analyzing the field measurement data, by which information was extracted and used in establishing a prediction model. From a *one-third octave band* analysis of the experimental data obtained, they observed the existence of two peak levels in the frequency domain. One has a fixed value corresponding to the tunnel/soil natural frequency, and the other has a value that increases with the train speed corresponding to the *sleeper passing frequency* f_s, that is,

$$f_s = \frac{c}{l_s}, \tag{1.22}$$

where c is the train speed and l_s the spacing between sleepers. Whenever the two peak frequencies coincide at certain train speed, the vibration level will increase drastically due to the effect of *resonance*.

From the analysis of some measurement data, remarks were made by Heckl *et al.* (1996) concerning the mechanism of vibrations excited by the moving trains. They found that besides the sleeper passing frequency f_s, the *wheel passing frequency* f_a is another crucial parameter for the vibrations induced by moving trains. Here, the wheel passing frequency f_a is defined as

$$f_a = \frac{c}{l_a}, \tag{1.23}$$

in which l_a is the distance between two consecutive wheels. Since the distance between two consecutive wheels is generally not constant for a commercial train, the wheel passing frequency is less apparent than the sleeper passing frequency. Other possible excitation mechanisms of ground vibrations by moving trains include the *quasi-static pressure* generated by the wheel axles onto the track, the effects of joints in unwelded rails, unevenness of wheels or rails, and the effects of carriage- and wheel-axle bending vibrations associated with their natural frequencies (Krylov and Ferguson, 1994).

Volberg (1983) carried out measurements of vibration propagation induced by passing trains at three different sites with different ground properties. The measured data appear to be rather independent of the sites investigated. A calculation scheme involving a simple power law was proposed for predicting the train-induced vibrations in the vicinity of planned railroad tracks. Noise and vibration measurements have been conducted for the rapid rail transit system in Calcutta, India by Mohanan *et al.* (1989). The results of measurement showed that both the noise and vibration levels were higher than the recommended values. Based on these data, the factors influencing the results were discussed and the methods for reducing the noise and vibration levels were proposed. With reference primarily to the *German standards*, Kurze (1996) reviewed various measurement procedures and prediction schemes in use for determining the environmental impact of railway noise and vibration. Common methods for noise and vibration control at sources and in the propagation paths were also discussed in this paper.

In China, experimental measurements were carried out for a tunnel in *Beijing subways* by Pan and Xie (1990). Two in-situ experiments were performed for a bridge site and buildings near the railway lines by Xia *et al*. (2005) concerning the vibrations induced by running trains. In Japan, Okumura and Kuno (1991) studied the effects of various factors on the railway noise and vibration through a regression analysis of the field data collected for 79 sites along 8 traditional railway lines in an urban area. Among the six factors they used to explain the vibration peak level, i.e., the distance, railway structure, train type, train speed, train length and background vibration, they found the influence of distance to be most crucial. The second prominent factor is background vibration, which is considered to be characteristic of the soil properties at each site. They also found that the influence of train speed is not so obvious. Such an observation can be attributed to the fact that the field data is collected from traditional railways, whose running speed is generally below 100 km/hr (27.77 m/s), far smaller than the R-wave speed for usual soil conditions. Regarding the influence of railway structures, the vibration levels for the concrete bridges and retaining walls are lower than those for the at-grade structures.

Takemiya (1998a) analyzed the measured field data alongside one *Shinkansen railway* during the train passage, which has an average speed of around 240 km/hr. He concluded that the high-speed train generates rather impulsive ground motions of short duration corresponding well with the wheel distance. Consequently, the vibration property can be modeled quite well, given the information of wheel distance and the number of carriages connected. From his observation, the response features are significantly different for different types of supporting structures. For instance, much more waves are reflected through the layered soils for the at-grade track, while for railways of the viaduct type, the frequency contents of the structure-borne vibration are closely related to the soil-structure system.

Lang (1988) performed some experiments to test the effectiveness of floating concrete slabs and trenches in isolating the vibrations of buildings located near the railway track. The results indicate that both methods are effective for reducing the vibrations, but the barriers appear to be more effective for reducing the vibrations if they are installed at places closer to the track.

Recently, a project named *CONVURT* (Clouteau *et al.*, 2005) was conducted by the European Union, aimed at controlling the vibrations generated by underground rail traffic through a multi-national effort. Within the framework of this project, Chatterjee *et al.* (2003) and Degrande *et al.* (2006a) performed in-situ vibration measurements in Paris and London, respectively.

1.4 Empirical Prediction Models

Due to the lack of a proper understanding of the excitation generation mechanism from railway trains and the difficulty involved in determining the soil properties, to precisely model the soil-structure system of concern using existing numerical methods is not an easy task. In this regard, one feasible, but approximate, approach is to construct a simplified but reasonable model for predicting the responses based on the empirical and theoretical results available. By and large, most prediction models existing in the literature are composed of several separable independent formulas, each of which contains a control parameter and can affect to a certain extent the final response. A simple prediction model such as this can be used to provide tentative estimates, when extensive measurements or investigations are not affordable or cannot be achieved in a short time.

Gutowski and Dym (1976) and Verhas (1979) combined the essence of measurement and theory into a predictive model, which is given in a simplified form of *attenuation function*, taking into account the effects of material attenuation and geometrical attenuation. Kurzweil (1979) presented a model for predicting the vibration of buildings caused by the trains passing nearby, in which the vibration attenuation due to propagation through the ground, the ground-building interaction, and the propagation characteristics of the building were all taken into account. Melke (1988) proposed a procedure for predicting the structure-borne noise and vibration from underground railway lines. Based on the analytical techniques and laboratory measurements, a chain of *transmission losses*, including the track transmission loss, tunnel transmission loss, ground transmission loss, and building transmission loss, was proposed to predict the final velocity level of the building. Trochides (1991) presented a simple method for predicting the excitation levels due to ground-borne vibrations in buildings located near the subways. This model is based on approximate impedance formulas for the tunnel and structure, as well as simple energy considerations. Comparisons between the calculations and measurements on scaled models showed that the predictions were generally acceptable for design purposes.

By the use of a statistical formulation, Madshus *et al.* (1996) proposed a semi-empirical model for predicting the low frequency vibrations, based on a large number of vibration measurements in Norway and Sweden. To make possible a unified and systematic handling of the empirical data, a database was established, too. This model includes five separable statistically independent factors, i.e., the train type specific vibration level, speed factor, distance factor, track quality factor, and building amplification factor. In order to minimize the negative influence of vibrations in buildings located near railways, *Swiss Federal Railways* developed a three-part computer program for predicting the emission of vibrations and structure-borne noises for every newly constructed or extended railway track (Kuppelwieser and Ziegler, 1996). Recently, a simple prediction model specially tailored for the *Italian high-speed railway* was proposed by Rossi and Nicolini (2003).

1.5 Numerical Simulation

Concerning the literature on ground-borne vibrations, most of the early researches were conducted by analytical or experimental approaches. Whenever an analytical approach was adopted, however, restrictions were often imposed on the geometry and material properties of the problem considered, as closed-form solutions cannot be easily made available for most practical situations. On the other hand, although the results obtained by the experimental approaches appear to be most reliable and close to real situations, an exhausted field test may cost a lot. Starting from the mid 1970s and enhanced by the advent of high-performance computers, various numerical methods emerged as effective tools for solving the wave propagation problems, including in particular the finite element method, boundary element method, and their variants.

In the past three decades, a great portion of the studies on wave propagation problems were performed by the *boundary element method*. A significant amount of the relevant works can be found in the review papers by Beskos (1987, 1997). Using the boundary element method, the *radiation damping* can be accurately taken into account through use of suitable fundamental solutions. However, the irregularities in geometry

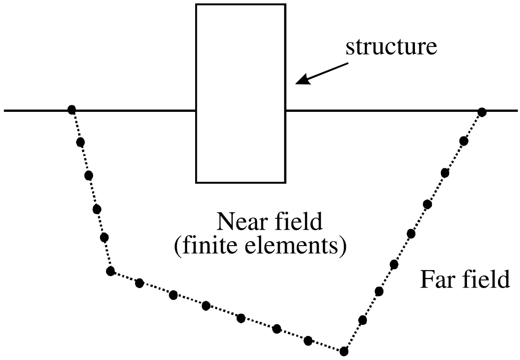

Fig. 1.5 Schematic diagram of the hybrid method.

and materials of the structure and underlying soils, as may be encountered in practice, cannot be dealt with in an easy way. It is true that some modern versions of the boundary element method have also been equipped with the capability to deal with the inhomogeneity in geometry. Nevertheless, this has been achieved at the expense of using a much more complicated *Green's function* or a finer subdivision of the interior domain considered.

In contrast, the finite element method appears to be more versatile in applications, with which various irregularities in geometry, including the embedded structures and multi soil layers, can be simulated with no difficulty. Thus, as far as the vibration of structures and surrounding soils is concerned, a finite element modeling remains the most favorable choice. However, the finite element method suffers from the drawback that the soil, which is semi-infinite by nature, can only be modeled by elements of finite size. Consequently, the *radiation damping* that accounts for the loss of energy due to waves traveling to infinity cannot be accurately modeled.

To overcome this drawback, other auxiliary methods are often called for to model the infinite region, which leads to the so-called *hybrid method*. By this method, the domain of a soil-structure system is divided into two sub-domains, i.e., the *near field* and *far field* (Fig. 1.5). The near field consisting of the structure and the region of the soil of interest, as enclosed by the dotted line in the figure, is modeled by the finite elements as conventional. The far field is a semi-infinite domain excluding the near field. The dotted line in the figure can be regarded as the interface between the near and far fields. In a finite element analysis, the *impedance matrix* for the far field is established in terms of the nodal points at the interface, as indicated by the dotted line, for relating the nodal forces to the nodal displacements.

In the literature, a number of methods exist for modeling the infinity property of the far field for use in the finite element simulation, which include, for instance, the traditional boundary element method, consistent boundary, transmitting boundary, viscous boundary, superposition boundary, paraxial boundary, double-asymptotic boundary, extrapolation boundary, multi-direction boundary, infinite element, and the so-called consistent infinitesimal finite-element cell method. A discussion of the advantages and disadvantages of each of these methods can be found in Wolf and Song (1996), which will not be recapitulated here.

Owing to its flexibility, the *hybrid method* has often been used in dealing with problems involving the wave barriers, buildings, embankment, layered soils, as well as rails and tracks. In general, there are three approaches for modeling the half-space problems: two-dimensional (2D) modeling, three-dimensional (3D) modeling, and two-point-five-dimensional (2.5D) modeling. By the coupled finite element-boundary element method, Andersen and Jones (2006) investigated the quality of the results obtained from the 2D model of a railway tunnel through comparison with those obtained from a corresponding 3D model. They concluded that 3D models are required for absolute predictions. However, the 2D model provides results that agree qualitatively with those of the 3D model at most frequencies. Consequently, for problems of which the qualitative behavior, rather than the quantitative behavior, is of primary concern, a 2D model is considered sufficient.

Intuitively, the results obtained by 3D modeling are believed to be most trustworthy. Following general finite element analysis procedures, one can establish the 3D model for simulating the structure of concern and surrounding soils in a straightforward manner, and then use such a model to analyze the dynamic response of the structure-soil system. A major concern in this regard is the large effort required in establishing the three-dimensional analysis model and the huge amount of computation required for the frequency-domain analysis, which may involve the operations of complex numbers.

Zhao and Valliappan (1993) presented a dynamic infinite element for 3D infinite-domain wave problems. Park *et al.* (2004) developed 3D elastodynamic infinite elements for soil-structure interaction problems. As far as the practical applications are concerned, a 3D finite element analysis was conducted by Ju (2002) for the ground vibration due to trains moving over a seven-span bridges, using the absorbing boundary conditions to simulate the infinite boundary of the soils. The dynamic 3D finite element program ABAQUS was adopted by Hall (2003) to simulate the train-induced ground vibrations with the boundary simulated by a number of dashpots. However, as was pointed out by both authors, a full 3D dynamic finite element analysis of the half-space problem is extremely time-consuming. For this reason, only a limited amount of research works have been carried out along these lines of research for ground-borne vibrations. It is realized that for problems with great variations in the geometric and material properties of the soil-structure system, a full 3D finite element modeling may still be necessary, in order to capture some of the local effects that may be hidden by the 2D or other simplified models.

Fortunately, due to the periodic nature of the loading and geometry of the half-space along the direction of the moving loads, a third type of modeling called the *2.5D modeling* has been made possible for simulating the 3D problem. By the 2.5D approach, one uses a finite element mesh that is basically of the 2D nature, but with due account taken of the load-moving effect in the third dimension, to simulate the 3D dynamic behavior of the half-space. Based on the above discussions, only a brief review of the 2D and 2.5D modeling will be given in the following.

1.5.1 *Two-dimensional modeling*

A survey of the literature indicates that most early researches on the ground-borne vibrations were based on the two-dimensional modeling with *plane strain* assumption. Under the condition that the external loading can be regarded as an *infinite line load*, and that the material and geometric properties of the system are identical along the direction of the line load, the assumption of plane strain applies and therefore the two-dimensional modeling can be adopted. According to Gutowski and Dym (1976), the passage of train loads can be reasonably simulated as a moving line load, provided that the receiver from the track is approximately less than $1/\pi$ times the length of the train.

Segol *et al.* (1978) used finite elements along with special non-reflecting boundaries to investigate the isolation efficiency of open and in-filled trenches in layered soils. Balendra *et al.* (1989) used finite elements along with the viscous boundary to investigate the vibration of a subway-soil-building system in Singapore. Thiede and Natke (1991) adopted a similar method to study the influence of thickness variation of subway walls. Laghrouche and Le Houedec (1994) used finite elements along with consistent boundaries to study the effectiveness of an elastic mattress lying under a railway in reducing the traffic-induced ground vibrations. Chua *et al.* (1995) analyzed a subway-soil-building system using a two-dimensional finite-element idealization, in conjunction with an analytical derivation of the train-loading spectrum at the tunnel invert. Yang *et al.* (1996) and Yang and Hung (1997) combined the finite and infinite elements to investigate the effect of trenches and elastic foundation in reducing the ground vibrations induced by moving trains. Hung *et al.* (2001) used the same procedure to study the vibration of the building alongside the railway. Analytical frequency-dependent infinite elements were presented by Yun *et al.* (2000) and Kim and Yun (2000) for analysis of 2D soil-structure systems.

1.5.2 *2.5-dimensional modeling*

For practical reasons, one may assume that the material and geometric properties are identical along the direction of a railway track. Consider a 2D profile perpendicular to the track, which consists of the cross section of the railway, surrounding soils and even the bedrock. If the load-moving effect in the third dimension is not of concern, then the use of the 2D profile including the geometric and material variations of the half-space is generally sufficient.

However, if the effect of load-moving in the third dimension is to be considered, then the use of the 2D profile alone is not sufficient. This is especially true when the train speed increases and approaches the critical speed of the soil, as the *Mach radiation* effect of the soil cannot be ignored. In reality, such a problem is two-dimensional in geometry, but three-dimensional in wave propagation. Strictly speaking, it can be analyzed only using a 3D model. However, for problems where the geometry and material properties are uniform along the railway direction, the use of a 3D model to simulate a problem that is 2D in nature is not computationally efficient.

By taking into account the relation of displacements between two nodes on the neighboring finite elements along the direction of wave-traveling, a solid element was reduced to a plane element with three degrees of freedom per node by Hwang and Lysmer (1981). This element was used to study the response of underground structures under the traveling seismic waves. A similar idea called the *dimensionality reduction* was later employed by Luco and de Barros (1994, 1995) to study the seismic response of a cylindrical shell and a layered cylindrical valley embedded in a layered half-space, and by Stamos and Beskos (1996) to study the seismic response of long lined tunnels excavated in a half-space.

As an extension of the work by Hwang and Lysmer (1981), the three-dimensional wave propagation behavior of traffic-induced vibrations was analyzed by Hanazato *et al.* (1991), in which the weights, speed, intervals, and vibrating conditions of the vehicles were all taken into account. The near field was modeled by finite elements, and the far field by thin-layered elements. Later, Takemiya (1997) used similar finite elements to model the embankment, while adopting the boundary element procedure to derive Green's function for the underlying layered soils by discretization along the depth.

As was stated previously, the problem of train-induced ground vibrations is two-dimensional in geometry, but three-dimensional in wave propagation. Thus, if the original 2D formulation can be modified to include the load-moving effect in the third dimension, then we can use basically the same 2D mesh to generate the 3D response of the problem considered. This has been the idea behind the 2.5D approach proposed by Hung (2000) and Yang and Hung (2001), which can also be regarded as an extension of the original 2D approach by Yang *et al.* (1996) for modeling the soil-structure system in the wave-number and frequency domain using the finite/infinite elements.

By the 2.5D approach, the geometry and material properties of the half-space along the load-moving direction are assumed to be invariant. An extra degree of freedom is introduced at each node to account for the out-of-plane wave transmission, in addition to the two in-plane degrees of freedom conventionally used for the plane strain element. The profile of the half-space is divided into a *near field* and a semi-infinite *far field*. The near field containing the acting loads, structures, and soil region of concern is simulated by finite elements, while the far field containing infinite soil domains by infinite elements. By first transforming the system equations to the frequency domain and then back to the time domain, the 2.5D finite/infinite element method can be used to simulate the three-dimensional wave traveling behavior of the soil-structure system due to the moving loads for all ranges of speeds considered. Later, the 2.5D approach was adopted by Yang *et al.* (2003) to study the wave propagation behavior of layered soils due to surface moving trains. The results from this study allow us to visually apprehend how the Mach cones are formed along the railway track as the train speed increases from the sub- to the super-critical speed range. The 2.5D approach was also adopted to study the reduction efficiency of various wave barriers by Hung (2000) and the ground vibrations caused by underground moving trains by Yang and Hung (2008).

Similarly, but not based on the finite/infinite element approach, Sheng *et al.* (2006) used the boundary element method incorporating the wave number in the track direction to predict ground vibrations from trains running on the ground surface and in tunnels. Recently, by the hypothesis that the tunnel and soil are periodic in the longitudinal direction of the tunnel, Degrande *et al.* (2006b) proposed a periodic coupled finite element-boundary element formulation for predicting the free-field vibrations caused by metro trains moving through the tunnels. By the periodicity assumption for the geometry, the discretization of the soil-tunnel system in the direction of the tunnel is limited to a single-bounded reference cell.

1.6 Isolation of Ground Vibrations

There have been a number of methods developed for the control of ground-borne vibrations due to moving trains. The most popular countermeasures include the installation of trenches, wave impeding barriers, and floating slab tracks. Depending on whether the isolation device is installed near the source of excitation or near the structure to be protected, the method of isolation can be classified as *active isolation* or *passive isolation*, respectively. In what follows, the major features and literature associated with each type of wave barriers will be discussed. Other possible methods of railway vibration reduction include the installation of very thick tunnel walls, resilient mount under buildings (Newland and Hunt, 1991), an increase in tunnel depth, rail grinding and wheel truing, or using rail pads, under-sleeper pads, ballast mats, etc. (Wilson *et al.*, 1983).

1.6.1 *Trenches*

The trenches, including open and in-filled ones, have been used as wave barriers for isolating the vibration of machine foundations for years. Relevant literature on this subject has been abundant. An experimental investigation on the screening effect of open trenches was performed by Woods (1968). By the lumped mass method, Lysmer and Waas (1972) studied the effectiveness of a trench in reducing the horizontal shear wave motion induced by a harmonic load acting on the rigid footing lying over a horizontal soil layer. Segol *et al.* (1978) used the finite elements, along with special *non-reflecting boundary*, to investigate the isolation efficiency of open and bentonite-slurry-filled trenches in layered soils. Yang and Hung (1997), Hung (2000), and Hung *et al.* (2004) used the 2D and 2.5D finite/infinite elements to parametrically analyze the isolation effect of open trenches, in-filled trenches, and elastic foundations. Other related works that should be cited here include those of Aboudi (1973), Emad and Manolis (1985), Beskos *et al.* (1986), Beskos *et al.* (1990), Ahmad and Al-Hussaini (1991), Ahmad *et al.* (1996), Ni *et al.* (1994), Al-Hussaini and Ahmad (1991, 1996), Yeh *et al.* (1997), and Ni and Hung (1998).

As indicated by the aforementioned works, the most important requirement for the trench to achieve a good effect of isolation is that the trench should have a depth of an order of the surface wave length. Primarily for this reason, the isolation of ground-borne vibrations by trenches is effective only for moderate to high frequency vibrations.

1.6.2 *Wave impeding block*

Because of the presence of a rigid rock base, a soil stratum has some intrinsic eigenmodes for the waves to transverse, according to Wolf (1985). No vibration eigenmodes can be induced below the *cut-off frequency* of the soil stratum, which equals $c_P/(4H)$ for the vertical injected longitudinal waves, and equals $c_S/(4H)$ for the shear waves, with H denoting the depth of the soil stratum. It is therefore possible to take advantage of this vibration transmission property of the soil layer over the bedrock to impede the spreading of vibrations, say, by installing an artificial stiff plate at a certain depth below the source. Such an idea has led to invention of the so-called *wave impedance barrier* (WIB) for vibration reduction. Among the works conducted on the subject, the following should be cited: Schmid *et al.* (1991), Antes and von Estorff (1994) and Takemiya and Fujiwara (1994). All of these studies show that the WIB can effectively reduce the ground-borne vibrations. If an *artificial bedrock* is used, the foundation and soil vibrations can be significantly reduced, but the propagation of waves into the surrounding area cannot be totally prevented (commonly known as the *leaking problem*) for two reasons. First, the artificial bedrock is limited in length. Second, the artificial bedrock may vibrate by itself, in violation of its role as a rigid base. The effectiveness of the artificial bedrock can be improved by enlarging its length and stiffness. Shielding of the building from soil vibrations can also be achieved by installing an artificial bedrock directly beneath the building.

From the construction point of view, a WIB with a rectangular shape requires a substantial amount of excavation of the soils before the concrete block can be poured and cast on site. To overcome this drawback, the rectangular WIB was later modified by Takemiya (1998b) to be of the X shape, and referred to as the X-WIB. Such a device can be constructed by the conventional soil improvement procedure on site through mixing and injecting the cement paste directly into the soils. More recently, another WIB named honeycomb WIB was presented by Takemiya (2004) for mitigating the vibration induced from a high-speed train viaduct with pile foundations.

1.6.3 *Floating slab track*

The floating slab tracks, which consist basically of the concrete slab track supported by resilient elements, have been widely used on modern rail transit systems (Wilson *et al.*, 1983). It is well known that greater effectiveness can be achieved for reducing the ground-borne vibration and noise at frequencies above $\sqrt{2}$ times the vertical *resonant frequency* of the floating slab system. However, as the frequency is close or equal to the resonant frequency, the vibration will be greatly amplified. The design of floating slab tracks is based on the assumption of a single-degree-of-freedom system, with the lumped mass determined as the summation of the mass of the floating slab and the unsprung mass of the train, and the spring stiffness determined solely from the supporting resilient pads. In order to raise the effectiveness of the floating slab track, namely, to lower the resonant frequency, the mass of the floating slab should be enlarged as much as possible, because the resilient pads should not be too soft to ensure rail stability under full axle loads. Such highly resilient elements can be incorporated in different places of the transmission path to reduce the level of vibrations. Many different devices can be used as the resilient elements, including the rubber springs under the rails, Cologne eggs (Esveld, 1989), ballast, resilient devices under sleepers, plates under the rails, foam rubber mats under the ballast, etc. (Heckl *et al.*, 1996).

Balendra *et al*. (1989) used a two-dimensional finite element model to compare the effects of two different supporting systems, the direct fixation and the one with a floating slab. It was found that the vibration levels for the *floating slab track system* exceed those of the *direct fixation track system* in the low frequency range. However, in the high frequency range, the floating slab track system behaves as an effective vibration isolator. Grootenhuis (1977) introduced several types of floating track slabs that were already used in engineering applications, while proposing a new design that can be constructed inside a bored tunnel without increase in the tunnel diameter. Wilson *et al.* (1983) also studied the effectiveness of a floating slab trackbed for a rapid transit system in Washington, D.C. Laghrouche and Le Houedec (1994) and Yang and Hung (1997) investigated the isolation efficiency of an *elastic foundation* in reducing the train-induced vibrations. In general, the function of an elastic foundation constructed right underneath the track is similar to that of the floating slab track. Nelson (1996) discussed some of the developments and applications of vibration mitigating measures taken at the vibration sources in the U.S.A. and Canada. According to this study, the best performance in terms of the vibration attenuation can be expected from the floating slab system, among those techniques implemented for the source.

1.7 Evaluation Criteria of Vibration

Many design guides and standards have offered methods for assessing or reducing human exposure to vibrations in buildings. The effect of vibration on comfort and annoyance, however, is a very complex issue and cannot be specified solely by the magnitude of monitored vibrations alone. In other words, vibration associated phenomena, such as structure-borne noise, airborne noise, rattling, movement of furniture and other objects, as well as visual effects, may relate to the degree of complaints. Some studies, including the works done by Howarth and Griffin (1991), Paulsen and Kastka (1995), and Knall (1996), have been conducted to predict the subjective response of human beings to simultaneous noise and vibration produced in buildings located alongside the railways. It was concluded that for a proper evaluation of annoyance, the combined effects of the noise and vibration should be taken into account, rather than either the noise or vibration alone. However, researches related to the combined effect of disturbances by noise and vibration are still insufficient to form a valid basis for implementation of design standards. Further investigations with field experiments are required to establish appropriate criteria for evaluation of human response to train-induced vibrations in buildings.

Table 1.1 Standards for evaluation of human exposure to vibration in buildings.

Nation	Name of Standard	Standard Number
International Organization for Standardization	International Standards	ISO 2631-1 ISO 2631-2
United States of America	American National Standards Institute	ANSI S3.29
United Kingdom	British Standards	BS 6472
Germany	Deutsches Institut für Normung	DIN 4150-2
Norway	Norwegian Standard	NS 8176
Japan	Japanese Industrial Standards	JIS C 1510 JIS Z 8735

Experience in many countries has indicated that the occupants of residential buildings are likely to complain even if the vibration levels only slightly exceed the perception threshold, which for instance may range from about 0.01 to 0.02 m/s^2 peak, according to the *International Standards* ISO 2631-1:1997 (1997). Therefore, most standards provide values representing approximately the same human response with respect to annoyance of various frequencies, but no acceptable magnitudes on the building vibrations alone. Table 1.1 lists the standards used in some countries. Most standards for the evaluation criteria of vibrations, for example, the *Norwegian Standard* NS 8176 (Turunen-Rise *et al.*, 2003), contain two main objectives. The first is to define a unified method for measuring and quantifying vibrations, and the second to give some limit criteria for vibrations.

The International Standards ISO 2631-2 is the most commonly used standards and has often been regarded as the basis of other standards for development of related criteria for evaluating the human exposure to vibrations in buildings. A brief conceptual review of such a standard will be given in the following. For those who are interested in applications of the vibration criteria for buildings, this standard should be consulted for more details. As the part of the standards to be summarized below is related to assessment of public vibration nuisance, it should find applications to ground-borne vibrations induced by the moving trains as well.

The International Standards ISO 2631-2 is a part of ISO 2631, which offers guidance on the evaluation of human exposure to whole-body vibrations, especially for vibrations in buildings from 1 to 80 Hz. The measurement of vibrations should follow the methods given in ISO 2631-1. As human sensitivity to vibration is highly frequency-dependant, the summation effects should be considered for vibrations of different frequencies. Thus, overall weighted vibration values in terms of acceleration are often used in the evaluation. The *frequency-weighted acceleration* a_ω is determined by appropriate weighting and addition of one-third octave band data as follows:

$$a_\omega = \left[\sum_i \left(\omega_i a_i \right)^2 \right]^{1/2}, \tag{1.24}$$

where ω_i is the weighting factor for the *i*th one-third octave band and a_i is the root-mean-square (r.m.s.) acceleration for the *i*th one-third octave. The frequency weighting is normally incorporated in the design of measuring equipment with built-in weighting filters and band-limiting filters. Most modern vibration meters give an overall level of frequency-weighted acceleration on the measured axis a_ω. For brevity, the values of the frequency weighting factors will not be listed here. Those who are interested in calculation of the frequency-weighted acceleration should refer to the standard ISO 2631-1:1997 (1997) for further details.

The basic evaluation parameter given in ISO 2631-1:1997 (1997) is the *weighted r.m.s. acceleration* a_ω (in m/s^2 or rad/s^2), defined as

$$a_\omega = \left[\frac{1}{T} \int_{t=0}^{T} a_\omega^2(t) dt \right]^{1/2}, \tag{1.25}$$

where T is the duration of measurement (s). The weighted r.m.s. acceleration a_ω should be determined for each axis (x, y and z) of the principal surface of the floor supporting the human body. For undefined axis of human vibration exposure, the combined effects of vibrations in buildings are also taken into account by the combined standard base curve shown in Fig. 1.6.

According to the ISO 2631-2:1989 (1989), satisfactory vibration magnitudes for rooms of various functions should be specified in multiples of the base curve magnitudes. The ranges of multiplying

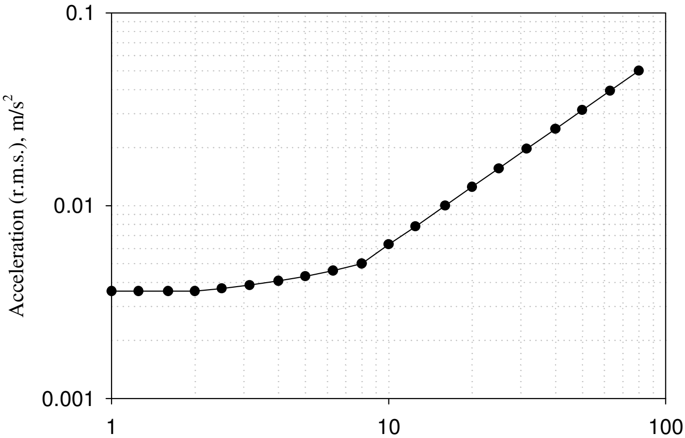

Fig. 1.6 Combined direction (*x*-, *y*-, *z*-axis) acceleration base curve for building vibrations: ISO 2631-2:1989.

Table 1.2 Multiplying factors given for vibration magnitudes below which the probability of adverse human reaction is low (ISO 2631-2:1989).

Place	Time	Continuous or intermittent vibration	Transient vibration excitation with several occurrences per day
Critical working areas (e.g. some hospital, operating theatres, some precision laboratories, etc.)	Day Night	1	1
Residential	Day Night	2 to 4 1.4	30 to 90 1.4 to 20
Office	Day Night	4	60 to 128
Workshop	Day Night	8	90 to 128

factors used in several countries were listed in Table 1.2. Complaints are likely to arise from the occupants of buildings when the vibration magnitudes, i.e., the weighted r.m.s. accelerations, exceed the value represented by the corresponding curve related to each axis. This does not necessarily mean that the values above this curve will give rise to

Table 1.3 VDV suggested above which adverse reactions may be expected from residential building occupants (unit: $m/s^{1.75}$) (BS 6472:1992).

Place	Low probability of adverse comment	Adverse comment possible	Adverse comment probable
Residential buildings 16 hours (Day)	0.2 to 0.4	0.4 to 0.8	0.8 to 1.6
Residential buildings 8 hours (Night)	0.13	0.26	0.51

adverse reactions, as the magnitude which is considered to be satisfactory depends on the real circumstance.

According to Griffin's (1996) comprehensive handbook for human vibration, the *Vibration Dose Value* (VDV) is a preferred measurement unit for assessment of human exposure to railway vibrations, which is evaluated at the center of the floor of interest during the measurement period. The VDV is used as a measure of the cumulative exposure to vibrations from a passing train, and also as one of the defined means for assessing the vibration severity in ISO 2631-1:1997 (1997). It is defined as the fourth root of the integral of the fourth power of the frequency-weighted acceleration a_ω over a period T:

$$\text{VDV} = \left[\int_{t=0}^{T} a_\omega^4(t)dt \right]^{1/4}, \tag{1.26}$$

where $a_\omega(t)$ is the *instantaneous frequency-weighted acceleration* (m/s^2) or (rad/s^2) and T is the duration of measurement (s). The SI unit of VDV is $m/s^{1.75}$.

In general, the *British Standards* BS 6472:1992 (1992) is quite similar to ISO 2631-2:1989 (1989). Besides the frequency-weighted r.m.s. acceleration, the VDV is used by the BS 6472:1992 (1992) as another measurement for evaluation of the human response to vibrations in buildings. Examples for calculating the VDV were given in this standard. Table 1.3 lists the VDV suggested by BS 6472:1992 (1992), in which the ranges for adverse reactions expected from residential building occupants were also listed.

In the newest edition of ISO 2631-2:2003 (2003), the baseline curves are not used any more. This edition gives only measurement methods for vibration, while the same guidance as in ISO 2631-1:1997 (1997) is adopted for evaluating the annoyance of human beings. In this standard, it was pointed out that complaints of occupants of residential buildings are likely to arise if the vibration magnitudes evaluated in terms of the frequency-weighted r.m.s. acceleration slightly exceed the perception threshold extended from about 0.01 to 0.02 m/s^2 peak. Due to the lack of comprehensive understanding of vibration associated annoyance, collecting data for evaluation of the human response to building vibrations is encouraged for updating the future version of ISO 2631-2.

Another frequently used measurement of vibration is the *vibration acceleration level* L_{va} with unit decibel (dB), which is defined as

$$L_{va} = 20 \log \frac{a}{a_0}, \tag{1.27}$$

where a is the r.m.s. value of the vibration acceleration and a_0 is the reference vibration acceleration, which is taken as 10^{-5} m/s^2 by the *Japanese Industrial Standards* (JIS). If the perception threshold of human being is 0.01 m/s^2, the vibration acceleration level of the perception threshold is 60 dB. When the r.m.s. vibration acceleration is weighted, another definition of vibration measurement often used is the *vibration level* L_v with unit decibel (dB), which is defined as

$$L_v = 20 \log \frac{a_c}{a_0}, \tag{1.28}$$

where a_c is the r.m.s. value of the vibration acceleration weighted by the vertical or horizontal characteristics, and a_0 is the reference vibration acceleration (10^{-5} m/s^2 for JIS).

In Japan, the methods of measurement for vibration levels, especially for the ground vibrations due to public vibration nuisance, were standardized in JIS Z 8735 (1981) and JIS C 1510 (1995) for vibration level meters. The ground vibration caused by road traffic, factory facilities and construction work have been regulated by law so to protect the quality of life environment. The *Vibration Regulation Law* issued by the Ministry of the Environment (1976), Japan, applies to vibrations measured on the ground surface. Owing to the fact that people are more sensitive to vertical than horizontal vibrations in the frequency range of

Table 1.4 Vibration criteria regulated by the Vibration Regulation Law.

		Day	Night
Type I	Residential area	65 dB	60 dB
Type II	Commercial area Industrial area	70 dB	65 dB

Note: The criteria for the area within 50 m away from schools, hospitals, libraries and sanatoria are obtained with a reduction of 5 dB from the values listed above.

vibration nuisances and that the vertical ground vibration is usually more serious than the horizontal ground vibration, the focus of vibration impact assessment is placed mainly on the vertical vibration. The criteria of vibrations listed in the vibration regulation law have been reproduced in Table 1.4. The magnitude of vibration on the floor of a house is usually estimated by adding a value of 5 dB to the one measured on the nearby ground surface (Yokota, 1996). However, this correction value was obtained 20 years ago when most of the houses were made of wood. Nowadays, further researches on this subject are conducted to achieve a more reasonable value for modern buildings in Japan, which are made mainly of steel or reinforced concrete.

1.8 Concluding Remarks

An overall review arranged in an approach-oriented manner has been presented on the vibration issues associated with railways. Also commented are the countermeasures for vibration mitigation and evaluation criteria of vibration. Regardless of which approach was used, all the papers cited play a role in advancing the research on this subject.

The theoretical results serve as a useful reference for development of the other methods. By the analytical approaches, the major factors affecting each problem, such as the train speed, distance, and soil condition, can be identified, and guidelines for evaluating the relative influence of each of the factors can be drawn.

To perform a complete field measurement for the train-induced vibrations is always costly and labor-intensive, not only because the related equipment may not always be available, but because it is difficult to find a site with tracks and scheduled trains that is safe and convenient for testing. For the reasons stated, a database compiled from the field measurements is highly valuable. It can offer clues for evaluating the key factors involved in the overall dynamic response, such as the spacing of sleepers, spacing of wheels, unsprung masses, and the type of track supporting structures.

Empirical prediction models seem to be the roughest among the four approaches considered. But they offer a hands-on approach for engineers to draw a quick estimate when there is a lack of time for tedious numerical analysis and extensive field measurement.

With the rapid advancement of high-performance computers, numerical simulation emerges as a very effective tool for modeling the wave propagation problems. As a matter of fact, for many practical problems, the numerical approach remains the only approach that can be undertaken at a reasonably low cost and within a short period. Nevertheless, the reliability of numerical simulation in predicting the vibration levels depends largely on the accuracy of the input data and the choice of an appropriate theoretical framework, which can be evaluated using some benchmark problems through comparison with experimental or theoretical results previously made available.

The most complex process among the four processes mentioned in Sec. 1.1 for vibration transmission is the source generation mechanism. In the literature, most researchers considered only the effect of quasi-static pressure generated by the axle loads. But in reality, there may exist dynamic terms which may be generated by the unevenness of the wheels and rails, or associated with the sleeper passing frequency, rail passing frequency, and resonance in the vehicle suspension. All these factors should be taken into account in future studies.

From the analytical studies, we know that if a train travels at a speed greater than the propagation speed of the ground waves, a shock wave will be generated on the ground. Such a phenomenon should not be regarded merely as one of mathematical interest. It may arise in the real world due to the continuous rise in the operation speed of modern high-speed trains. For example, it was reported that train speeds over 500 km/hr have been achieved on an experimental track in France (Krylov, 1995). In May 1990, nine runs of TGV trains moving at speeds over 500 km/hr or 138.8 m/s were made by the *French Railway Company* (SNCF) on the section of track between Courtalain and Tours. More recently, according to a news released by SNCF on April 3, 2007, their new test train achieved a record-high speed of 574.8 km/hr in one of their eastern railway lines. These speeds have already surpassed the speed of Rayleigh waves of the sustaining soils. As a result, significant radiation effect on the ground vibrations became visible in these areas and has resulted in restriction of the speed for the TGV trains on that part of track (Dieterman and Metrikine, 1996). Measurements by the railway companies in Swiss (SBB), France (SNCF), Germany (DB), Holland (NS) and Great Britain (BR) have also confirmed the amplification of the vertical movement in the track when the train moves with a speed of the same order as that of the Rayleigh wave speed of the subsoil (Dieterman and Metrikine, 1997).

Of the previous works concerning the trans-Rayleigh wave behavior, most were conducted by theoretical investigations. However, as this phenomenon is becoming not merely as a theoretical issue, but can really take place in certain circumstances, much more realistic models should be adopted to thoroughly study such an effect, at least through in-depth numerical simulations. On the other hand, apart from passively setting a speed limit on the train and/or improving the supporting strength of the subsoil, few countermeasures have been proposed for vibration reduction of trains moving over critical speeds. As far as the trains moving at super-critical speeds is concerned, it is suggested that further research be conducted to investigate the stability of the track system, including the rails, and that the effectiveness of conventional wave barriers, including those mentioned in Sec. 1.6, be re-examined.

This review is conducted with the hope that it may provide useful information to engineers and researchers for evaluation of the environmental vibrations associated with high-speed railways and subways in different parts of the world. Besides, the papers cited herein serve as good references for further investigation.